Defining the Epitope Region of a Peptide from the *Streptomyces coelicolor* Phosphoenolpyruvate:Sugar Phosphotransferase System Able to Bind to the Enzyme I

Estefanía Hurtado-Gómez,* Olga Abián,[†‡] F. Javier Muñoz,[§] María José Hernáiz,[§‡¶] Adrián Velázquez-Campoy,[†] and José L. Neira*[†]

*Instituto de Biología Molecular y Celular, Universidad Miguel Hernández, 03202 Elche (Alicante), Spain; [†]Instituto de Biocomputación y Física de los Sistemas Complejos, Corona de Aragón, 42, 50009 Zaragoza, Spain; [‡]H. C. U. Lozano-Blesa, Instituto Aragonés de Ciencias de la Salud (I+CS-CIBEREHD), Avda. S. Juan Bosco, 15, 50009 Zaragoza, Spain; [§]Grupo de Biotransformaciones, Departamento de Química Orgánica y Farmacéutica, Facultad de Farmacia, Universidad Complutense de Madrid, 28040 Madrid, Spain; and [¶]Servicio de Interacciones Moleculares, Parque Científico de Madrid, 28040 Madrid, Spain

ABSTRACT The bacterial PEP:sugar PTS consists of a cascade of several proteins involved in the uptake and phosphorylation of carbohydrates, and in signal transduction pathways. Its uniqueness in bacteria makes the PTS a target for new antibacterial drugs. These drugs can be obtained from peptides or protein fragments able to interfere with the first reaction of the protein cascade: the phosphorylation of the HPr by the first enzyme, the so-called enzyme EI. To that end, we designed a peptide, HPr^{9-30}, spanning residues 9 to 30 of the intact HPr protein, containing the active site histidine (His-15) and the first α-helix of HPr of *Streptomyces coelicolor*, HPr^{sc}. By using fluorescence and circular dichroism, we first determined qualitatively that HPr^{sc} and HPr^{9-30} did bind to EI^{sc}, the enzyme EI from *S. coelicolor*. Then, we determined quantitatively the binding affinities of HPr^{9-30} and HPr^{sc} for EI^{sc} by using ITC and STD-NMR. The STD-NMR experiments indicate that the epitope region of HPr^{9-30} was formed by residues Leu-14, His-15, Ile-21, and Val-23. The binding reaction between EI^{sc} and HPr^{sc} is enthalpy driven and in other species is entropy driven; further, the affinity of HPr^{sc} for EI^{sc} was smaller than in other species. However, the affinity of HPr^{9-30} for EI^{sc} was only moderately lower than that of EI^{sc} for HPr^{sc}, suggesting that this peptide could be considered a promising hit compound for designing new inhibitors against the PTS.

INTRODUCTION

Bacterial pathogens are becoming resistant to the different antibiotics used to treat infectious diseases, a problem that is now becoming endemic worldwide (1). The majority of the antibiotics used today were discovered in the 1950s and 1960s. The pharmaceutical industry has been, since then, occupied in improving the activity of such compounds and in making them completely refractory to any resistance mechanism. During the 1990s, research into the bacterial genome triggered a resurgence of drug discovery with the use of high-throughput screening tools to identify new antibiotics. However, although many enzyme inhibitors have been discovered, only a few of them inhibit bacterial growth, and of those few, a small fraction has gone through clinical testing (2). On the other hand, during the same period of time, the analysis of bacterial genomes has led to important discoveries in the identification and interconnections of some metabolic pathways. The bacterial $PEP^{\perp}$-dependent sugar PTS is one of those: it is a multiprotein complex system that mediates the uptake and phosphorylation of carbohydrates and is involved in signal transduction (3,4). This system is present in bacteria but does not exist in animals or plants; thus, both its uniqueness and its involvement in several regulation steps make the PTS proteins essential for the bacterial survival and an ideal target for possible new antibacterial drugs (3,4).

The PTS involves a cascade of phosphoryl-transfer steps from PEP to sugar-specific enzyme II permeases via phosphointermediates of the general cytosolic non-sugar-specific phosphotransferase EI and HPr. EI, a dimeric protein, is autophosphorylated on a histidine residue by PEP (5), and then, the phosphoryl group is transferred to HPr. EI is one of the best conserved proteins in the prokaryotic kingdom, and it has no similarity to eukaryotic proteins. The non-sugar-specificity of EI and HPr makes both proteins excellent targets to control the function of the PTS; thus, any compound able to inhibit EI should interrupt the flow of phosphoryl groups along the cascade and, concomitantly, the use of HPr in the utilization of alternative carbon sources (3). Our aim is to design peptides or protein fragments derived from HPr able to interrupt the phosphorylation step with EI.

Submitted November 27, 2007, and accepted for publication April 11, 2008.

Address reprint requests to Adrián Velázquez-Campoy, Instituto de Biocomputación y Física de los Sistemas Complejos, Corona de Aragón, 42, 50009 Zaragoza, Spain. Tel.: 34-976-562215; Fax: 34-976-562215; E-mail: adrianvc@unizar.es.; or José L. Neira, Instituto de Biología Molecular y Celular, Edificio Torregaitán, Universidad Miguel Hernández, Avda. del Ferrocaril s/n, 03202, Elche (Alicante), Spain. Tel.: 34-966658459. Fax: 34-966658758. E-mail: jlneira@umh.es.

Abbreviations used: PEP, phosphoenolpyruvate; CD, circular dichroism; EI^{sc}, enzyme I of *Streptomyces coelicolor*; EI^{ec}, enzyme I of *E. coli*; HPr^{ec}, histidine phosphocarrier protein of *Escherichia coli*; HPr^{sc}, histidine phosphocarrier protein of *Streptomyces coelicolor*; HPr^{9-30}, peptide comprising residues Gly-9 to Gly-30 of the intact HPr^{sc}; ITC, isothermal titration calorimetry; NMR, nuclear magnetic resonance; PTS, sugar phosphotransferase system; STD, saturation transfer difference; TFE, trifluoroethanol; TSP, sodium trimethylsilyl [2,2,3,3-$^2H_4$] propionate; UV, ultraviolet.

Editor: Doug Barrick.

0006-3495/08/08/1336/13 $2.00

doi: 10.1529/biophysj.107.126664

Streptomyces is a soil-dwelling actinomycete that grows on a variety of carbon sources. These actinomycetes are at the origin of approximately two-thirds of all natural antibiotics currently produced by the pharmaceutical industry. The complete genome of *Streptomyces coelicolor* has been sequenced, and it shows the largest number of genes found in any bacteria (6). The presence of the different components of the PTS in *S. coelicolor* has been reported, and the corresponding proteins have been cloned and expressed (7,8). There is a large homology between these PTS proteins and those of other antibiotic-resistant species, such as *Vibrio cholerae* and *Streptococcus pneumoniae* (3,7,8). We have undertaken an extensive description of the structures and conformational stabilities of the HPr^{sc} and EI^{sc} proteins (9–12). HPr^{sc} is a single polypeptide chain of 93 amino acids; it lacks cysteine and tyrosine residues, and it has one tryptophan and one phenylalanine. The structures of HPr proteins from several species have been described by NMR (13,14) and x-ray (15,16), and the NMR assignments of HPr^{sc} indicate that its structure is similar to that observed in other members of the HPr family (J. L. Neira, unpublished results). The regions of HPr^{ec} involved in the binding to EI^{ec} are the first two α-helices as well as the loop preceding the first α-helix and the turn after the second α-helix, as shown by x-ray and NMR studies of the protein complex (17,18).

In this article, we describe the binding of a peptide derived from HPr^{sc} ($HPr^{9–30}$), containing the active-site histidine, to EI^{sc}. We have also tested the binding of the intact HPr^{sc} to EI^{sc} to allow comparison with the values obtained with the peptide and with the affinities measured in other species (19–21). The affinity was measured by using two biophysical techniques, namely, STD-NMR and ITC. The two techniques provided identical results when a final EI^{sc} concentration of $\sim$10 μM was used: the apparent dissociation constants were in the range of hundreds of micromolar. Both techniques qualitatively agree in that the affinity of $HPr^{9–30}$ for EI^{sc} was slightly lower than that of HPr^{sc}, although it contains only 22 residues of the intact protein. We can also conclude, based on the NMR results, that most of the residues of the intact HPr^{sc} implicated in the binding to EI^{sc} are also involved in the binding of EI^{sc} to $HPr^{9–30}$, which interestingly becomes helical on binding. Further, on the basis of ITC experiments and on the value of the affinity constant, we can conclude that the peptide can be used as a hit compound to design new antibiotics, whose activity should also be checked in other species.

MATERIALS AND METHODS

Materials

Imidazole, Trizma acid, Trizma base, TFE, NaCl, and TSP were from Sigma (St. Louis, MO). β-Mercaptoethanol was from BioRad (Hercules, CA), and the Ni^{2+} resin was from Invitrogen (Carlsbad, CA). Standard suppliers were used for all other chemicals. Water was doubly deionized and purified on a Millipore (Billerica, MA) system.

Purification of HPr^{sc} and EI^{sc}

The HPr^{sc} clone, comprising residues 1 to 93, was kindly provided by Dr. F. Titgemeyer (Erlangen, Germany). The cloning vector contains a His_6-tag at the N-terminus end in frame with the first methionine (Met-1) of the protein. The stability and the structure of the His-tagged protein are the same as those of the cleaved protein (10). Protein was purified as described (9).

The EI^{sc} clone was also kindly provided by Dr. F. Titgemeyer. The cloning vector contains a His_6-tag at the N-terminus end in frame with the Met-1 of the protein. The EI^{sc} protein is 576 residues long, and we assumed that the His_6-tag did not alter the binding properties of the enzyme. Protein was purified as described (12).

Protein concentrations were calculated from the absorbance of a stock solution measured at 280 nm, using the extinction coefficients of model compounds (22).

Peptide design and synthesis

The $HPr^{9–30}$ peptide (Ac-GWAEGLHARPASIFVRAATATG-$CONH_2$) was derived from HPr^{sc}, spanning residues Gly-9 to Ala-30. Those amino acids belong to the first α-helix of HPr^{sc} (residues Ala-16 to Thr-27) plus the preceding loop containing the active-site histidine and three flanking residues on each side to avoid fraying effects. The N- and C-termini were acetylated and amidated, respectively, to avoid charge effects. The peptide was purchased from Zinsser Analytic (Frankfurt, Germany). The CAC peptide (see below) was purchased from Zinsser Analytic, and the two other peptides were obtained from Isogen Life Science (I Jsselstein, The Netherlands). Purity was assessed in all cases by mass spectrometry (MALDI-TOF) and HPLC chromatography and found to be larger than 95%. Peptide concentrations were determined by using the absorbance of the tryptophan or tyrosine residues present in each peptide (22).

Circular dichroism measurements

Although the optimum pH for the binding reaction is unknown, we carried out our quantitative and qualitative measurements at pH 7, similar to the pHs used in the binding of EI to HPr in other species (19–21).

Spectra were collected on a Jasco J810 (Tokyo, Japan) spectropolarimeter fitted with a thermostated cell holder and interfaced with a Peltier. The instrument was periodically calibrated with (+)-10-camphorsulfonic acid. Far-UV steady-state spectra were acquired at a scan speed of 50 nm/min with a response time of 4 s and averaged over four scans at 298 K. Spectra were acquired in a 0.1-cm-pathlength cell (Hellma, Plainview, NY), and they were corrected with the proper baseline. The samples were prepared in 100 mM Tris buffer (pH 7). The EI^{sc}, HPr^{sc}, and $HPr^{9–30}$ concentrations were 4 μM, 10 μM, and 10 μM, respectively.

Fluorescence measurements

Fluorescence spectra were collected in a Cary Eclipse spectrofluorometer (Varian, Palo Alto, CA) interfaced with a Peltier-thermostated multicell holder. The slit widths were 5 nm for both excitation and emission wavelengths. Excitation wavelengths were 280 and 295 nm; both wavelengths yielded the same results (data not shown). The signal was acquired every 1 s, and the wavelength increment was 1 nm. Experiments were acquired at 298 K, in a 1-cm-pathlength quartz cell (Hellma). The EI^{sc} concentration was 2 μM in buffer Tris (100 mM), and 2 μM of either $HPr^{9–30}$ or HPr^{sc} was added in each experiment.

Attempts to determine the affinity constant by either CD or fluorescence failed because of the small affinity constant (see below).

Quenching experiments aimed at detecting protein self-association of EI^{sc} under the protein concentrations used in this work were carried out as described (12). The EI^{sc} protein concentration was varied from 0.5 to 15 μM at pH 7 (50 mM Tris buffer). We have assumed that the dominant species in EI^{sc} is a monomer and/or a dimer, as in other EI proteins.

NMR spectroscopy

All NMR experiments were acquired at 283 K on an Avance Bruker DRX-500 spectrometer equipped with a triple resonance probe and z-pulse field gradients.

Homonuclear one- and two-dimensional NMR experiments were performed at pH 7, 50 mM phosphate buffer (uncorrected for deuterium isotope effects) in H_2O/D_2O (90%/10% v/v). TSP was used as the external chemical shift reference in the homonuclear experiments.

Two-dimensional NMR spectra of HPr^{9-30} (1 mM) in the presence of 8.6 μM of EI^{sc} were recorded in the phase-sensitive mode by using the States-TPPI method (23). All experiments were carried out with the WATERGATE pulse sequence for water suppression (24). Two-dimensional ^1H-^1H TOCSY spectra were recorded by using an MLEV-17 spin-lock sequence (25) with a mixing time of 80 ms. NOESY experiments were recorded with mixing times of 100 and 250 ms. Typically, spectra were acquired with 512 t_1 increments, 2048 data points, and a relaxation delay of 1 s. The spectral width was 6000 Hz in all cases. The spectra were processed using the BRUKER-XWINNMR software on a PC workstation. All spectra were zero-filled in the indirect dimension to 1024 data points, and a square sine bell window function was applied in both dimensions before Fourier transformation. Sequential assignments of the proton resonances of isolated HPr^{9-30} have been previously described (26). Assignments of the peptide were not modified in the presence of EI^{sc} under any of the conditions explored (in a concentration range of HPr^{9-30} from 12 to 250 μM).

In the STD experiments, a certain volume from a stock solution of the peptide (not larger than 5 mM) or the intact HPr^{sc} was dissolved in 500 μL of a solution containing EI^{sc} in 50 mM phosphate buffer (pH 7.0). Then, the HPr^{9-30}:EI^{sc} or HPr^{sc}:EI^{sc} protein ratio was varied in each experiment by keeping constant the concentration of EI^{sc}. The one-dimensional ^1H-STD-NMR (27–29) spectra of the HPr^{9-30}:EI^{sc} and HPr^{sc}:EI^{sc} complexes were recorded with 4000 to 8000 scans. Selective saturation of protein resonances was set at -3 ppm (on resonance); control experiments at this frequency showed that the entire protein can be saturated uniformly and then efficiently used for the STD-NMR technique; furthermore, this frequency is far away from the most upfield-shifted methyl protons of either HPr^{sc} or the HPr^{9-30}, such that no perturbation of these signals occurred by the selective shaped pulse.

The time dependence of the saturation transfer with saturation times ranging from 0.2 to 2.5 s showed that at least 1.5 s was needed for efficient saturation transfer from the EI^{sc} protein to the ligand (HPr^{sc} or HPr^{9-30}) protons (see Results). STD-NMR spectra were acquired by using a series of equally spaced 50-ms Gaussian-shaped pulses for selective saturation (30). The radio-frequency field strength of the Gaussian-shaped pulses was ~100 Hz, with a 1 ms delay between the pulses. Residual water signal was eliminated by using excitation-sculpting procedures (31). A spin-lock sequence was applied before the excitation-sculpting sequence to remove the signals of the EI^{sc} protein (32). The reference STD spectra were recorded with the off-resonance set at 30 ppm. Saturated spectra were subtracted from the reference spectra via phase cycling.

The following controls were carried out to ensure that the STD effects observed were caused by real saturation of EI^{sc}. STD-NMR experiments with on- and off-resonance frequencies set at -3 and 30 ppm, using a saturation time of 2 s, were carried out on isolated HPr^{9-30} at 2 mM concentration. No signals were present in the difference spectra, indicating that the effects observed in the presence of EI^{sc} resulted from true saturation transfer. Similar control experiments were carried out in a sample containing HPr^{sc}, where the most up-field-shifted protons appear at 0.4 ppm (J. L. Neira, unpublished results). No signals were present in the difference spectra.

To further check that the measured values of the dissociation constants were not caused by the absence of the protein phosphorylation, control STD experiments were also carried out in the presence of 2 mM PEP, 4 mM $MgCl_2$ (the natural effectors of EI^{sc}), and 100 μM of HPr^{9-30} (pH 6.8, phosphate buffer) or 100 μM of HPr^{sc}. No differences were observed in the signal intensity of selected protons when compared to those in the absence of the effectors (data not shown).

Because the affinity constant of the peptide was very small (see Results), we carried out three controls, with different peptides to rule out any possibility of unspecific binding of HPr^{9-30} to EI^{sc}. The first peptide was identified in a phage display study against EI^{cc} as being able to inhibit the growth of *E. coli* strains (33); its sequence is GLRFGKTRVHYLVLG-NH_2. The second peptide is able to bind to thioredoxin m from pea, and it is derived from the pea chloroplast fructose-1,6-biphosphatase; its sequence is ESLP-DYGDDSDDNTLGTEEQRSIVNVSQ-NH_2. The last peptide comes from the protein forming the capsid of HIV, and it has been able to dissociate the dimeric wild-type protein (34); its sequence is: Ac-EQASQEVKNWM-TETLLVQNA-NH_2. The on- and off-frequencies, and the rest of the parameters in the STD experiments were the same as those used with the HPr ligands. The EI^{sc} concentration was 12 μM, and the corresponding peptide concentration was ~2 mM in the three controls. The saturation time was 2 s in the three peptides.

To allow for comparison among the STD experiments, the signal intensities of the different protons were analyzed by the use of the fractional STD amplification factor, *STDaf*, which expresses the signal intensity in the STD spectrum, $I_0 - I_{sat}$, as a fraction of an unsaturated reference spectrum, I_0, and the excess of added HPr^{sc} or HPr^{9-30} peptide (27,28):

$$STD\ amplification\ factor(STDaf) = \frac{(I_0 - I_{sat})}{I_0} \times [HPr^{i}excess],$$

where $[HPr^i]$ is the concentration of either HPr^{sc} or HPr^{9-30} in each experiment. For the experiments with HPr^{9-30} the concentration of EI^{sc} was 8.6 μM (in monomer units), and for those with the intact HPr^{sc}, the EI^{sc} concentration was 10.3 μM (in monomer units). The errors in the *STDaf* were estimated from the determination of the STD effects measured in two identical samples at 1.5 s and processed simultaneously. The differences obtained were lower than 5% for all the measured resonances.

The apparent dissociation constant, K_D, was obtained by fitting the *STDaf* versus the concentration of added HPr^{9-30} or HPr^{sc} to:

$$STDaf_{meas} = STDaf^0 + \Delta STDaf_{max}\left(([EI] + [HPr^i] + K_D) - \sqrt{([EI] + [HPr^i] + K_D)^2 - 4[EI][HPr^i]}\right),$$

where $STDaf_{meas}$ is the *STDaf* measured at any particular concentration of HPr^{sc} or HPr^{9-30}; $STDaf^0$ is the value of the *STDaf* in the absence of HPr^{sc} or the peptide; $STDaf_{max}$ is the maximum of the STD effect; and [EI] is the concentration of EI^{sc} in the monomeric form (8.6 μM or 10.3 μM).

Fitting of data to the binding equation was carried out by a least-squares analysis using the program Kaleidagraph (Abelbeck software, Reading, PA) on a PC computer.

Isothermal titration calorimetry

ITC measurements were performed by using a VP-ITC isothermal titration calorimeter (Microcal, Northampton, MA). Measurements were carried out at 298 K. Sample cell (1.4 mL) was loaded with EI^{sc} at 20 μM; either HPr^{sc} or HPr^{9-30} was loaded into the syringe at a total concentration of 300 μM. Twenty-eight injections of 10 μL were added sequentially to the sample cell after 400 s to ensure that the titration peak returned to the baseline before the next injection. The amount of power required to maintain the reaction cell at constant temperature after each injection was monitored as a function of time. The obtained isotherms (differential heat upon binding versus the molar ratio: $[HPr^i]/[EI]$) were fitted to a single-site model assuming that the complex with EI^{sc} had a 1:1 stoichiometry (as described in other species (19)). Data were analyzed with software developed in our laboratory, implemented in the software package Origin 7.0 (Microcal). As a control experiment, the individual dilution heats for the intact HPr^{sc} were determined under the same experimental conditions by carrying out identical injections of the HPr^{sc} into

the sample cell, which contained only buffer. These control injections elicited no significant heat.

Experiments were carried out in two buffers to analyze the contribution of the buffer ionization enthalpy: 1), 12 mM Tris, pH 7.4, and 100 mM NaCl; and 2), 12 mM MOPS, pH 7.4, and 100 mM NaCl. Then, the apparent enthalpy change, $\Delta H_{\text{meas, buffer}}$, in the corresponding buffer is (35):

$$\Delta H_{\text{meas, buffer}} = \Delta H^0 + n_{\text{H}}\Delta H_{\text{ion}},$$

where ΔH^0 is the buffer-independent binding enthalpy, ΔH_{ion} is the ionization enthalpy of the buffer, and n_{H} is the number of exchanged protons between the complex and the solvent during the binding reaction.

RESULTS

Binding of EI^{sc} to HPr$^{9–30}$ and HPr^{sc} monitored by fluorescence and CD

The spectrum of EI^{sc} is characterized by an intense maximum at 335 nm (after excitation at either 280 or 295 nm), and its CD spectrum shows the features of an $\alpha + \beta$ helical protein (11,12). The fluorescence spectrum of HPr^{sc} shows also a maximum at 335 nm (after excitation at either 280 or 295 nm), as well as the features of an $\alpha + \beta$ helical protein in the far-UV CD (9). Conversely, the fluorescence spectrum of HPr$^{9–30}$ shows a maximum at 350 nm, and the CD spectrum resembles that of a random coil (26).

We carried out binding measurements by using steady-state fluorescence and CD with EI^{sc} and intact HPr^{sc}; differences were observed among the addition (CD or fluorescence) spectra and those of the corresponding complexes. The CD spectrum of HPr^{sc} (10 μM) in the presence of 4 μM of EI^{sc} is shown in Fig. 1 *B*. The spectrum corresponding to the addition of the spectra of EI^{sc} and HPr$^{9–30}$ is also different to that of the complex (Fig. 1 *D*). A similar behavior was observed when the emission fluorescence spectrum of the complex between EI^{sc} and HPr$^{9–30}$ was compared with the addition spectrum ob-

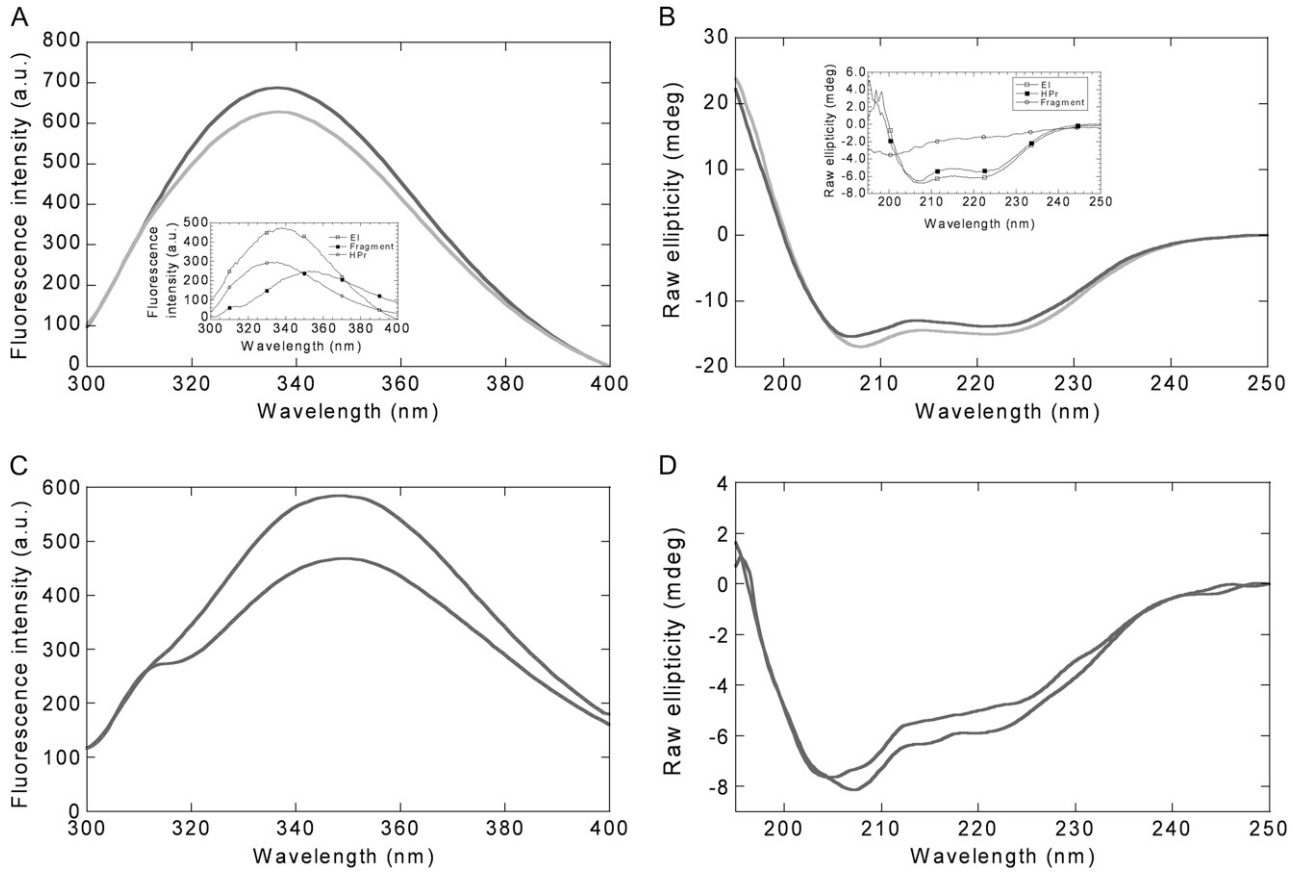

FIGURE 1 Binding of EI^{sc} to HPr^{sc} and HPr$^{9–30}$ measured by CD and fluorescence. (*A*) Fluorescence spectrum of the complex formed by HPr^{sc} and EI^{sc} (*light gray*) and that obtained by the addition of the spectra of both isolated species (*dark gray*). (*Inset*) Fluorescence spectra of HPr^{sc}, EI^{sc}, and HPr$^{9–30}$; the units on the *y* axis are arbitrary and cannot be compared with those of the main figure. (*B*) Far-UV CD spectrum of the complex formed by HPr^{sc} and EI^{sc} (*light gray*) and that obtained by the addition of the spectra of both isolated species (*dark gray*). (*Inset*) Far-UV CD spectra of HPr^{sc}, EI^{sc}, and HPr$^{9–30}$; the units on the *y* axis are arbitrary and cannot be compared with those of the main figure. (*C*) Fluorescence spectrum of the complex formed by HPr$^{9–30}$ and EI^{sc} (*dark gray*) and that obtained by the addition of the spectra of both isolated species (*light gray*). (*D*) Far-UV CD spectrum of the complex formed by HPr$^{9–30}$ and EI^{sc} (*dark gray*) and that obtained by the addition of the spectra of both isolated species (*light gray*). Conditions were 100 mM (phosphate buffer, pH 7) at 298 K, 2 μM EI^{sc}, and 2 μM of the corresponding ligand for the fluorescence spectra; similar results were obtained by excitation at 295 nm. In the far-UV experiments, the spectra were acquired at 278 K to increase the percentage of helical population in HPr$^{9–30}$, in 100 mM Tris buffer, pH 7, 4 μM EI^{sc} and 10 μM of the corresponding ligand.

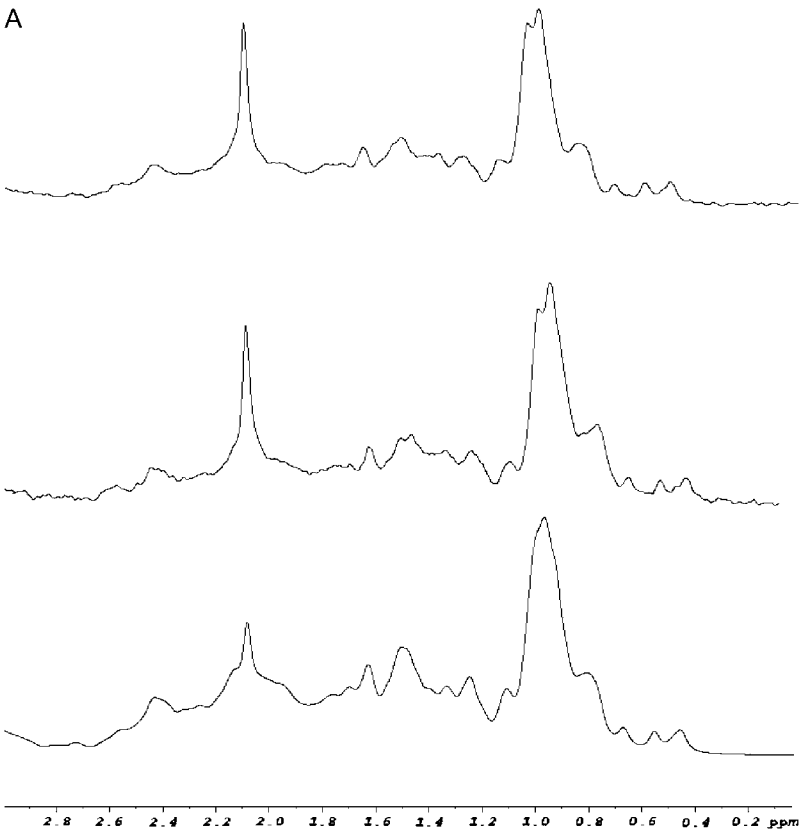

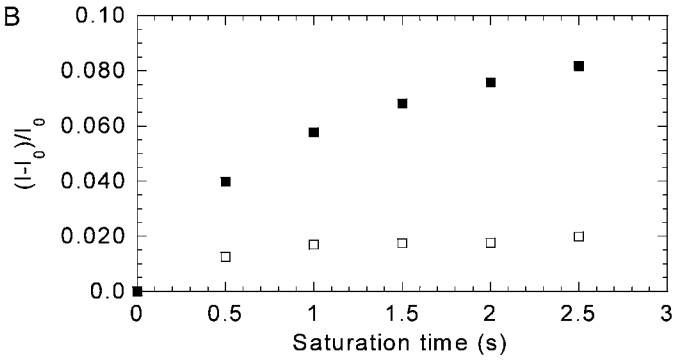

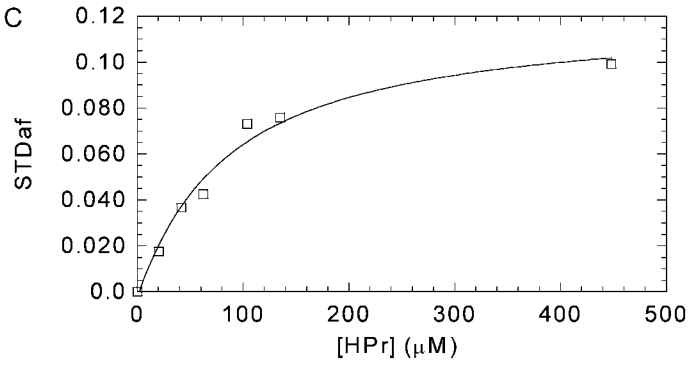

FIGURE 2 Binding of EI^{sc} to HPr^{sc} measured by STD-NMR. (*A*) STD-NMR spectra at different saturation times, from bottom to top: reference spectrum (*bottom*), STD spectrum at 1 s of saturation (*middle*), and at 2 s of saturation (*top*). (*B*) The rate between the methyl peak intensity in the STD spectra and that at the reference spectrum at 20.8 μM (*open squares*), and at 135.20 μM of HPr^{sc} (*solid squares*) are shown. (*C*) Binding curves for the *STDaf* of the methyl signals in HPr at 2 s of saturation time. The curve is the fitting of data to the equation of *STDaf*. Conditions were: 10.3 μM of EI^{sc} at 283 K.

tained by the sum of each isolated polypeptide chain (Fig. 1 *C*). These results suggest that, at least from a qualitative point of view, there is binding between either HPr^{9-30} or HPr^{sc}, and EI^{sc}. Taking into account the affinity constant determined by ITC and STD (see below), the amount of formed complex under these conditions should be ~10% in both HPr polypeptides, which should explain the differences observed.

To rule out the presence of a substantial amount of monomeric EI^{sc} species under our conditions, we monitored its self-association by using fluorescence quenching experiments and gel filtration measurements. We observed that at physiological pH, as the concentration of protein was increased, the value of K_{sv} (the Stern-Volmer constant) decreased: 1.3 ± 0.1 (at 0.5 μM), 0.96 ± 0.07 (at 1 μM), 0.92 ± 0.03 (at 2 μM), 0.8 ± 0.1 (at 4 μM of EI^{sc}), as previously reported (12); and, 0.85 ± 0.05 (at 8 μM), 0.81 ± 0.03 (at 10 μM), and 0.79 ± 0.05 (at 15 μM), as found in the extended range of explored protein concentrations in this work. We also carried out experiments at 15 μM of EI^{sc} of protein concentration by using an analytical gel filtration column (Superdex 200 HR 10/30, GE Healthcare, Piscataway, NJ), where the protein eluted at volumes corresponding to a molecular mass of 160 kDa (data not shown). Thus, under the conditions used in the CD, fluorescence, STD, and ITC measurements (see below), EI^{sc} remained dimeric.

Binding of EI^{sc} to HPr^{9-30} and HPr^{sc} monitored by STD-NMR

We first measured the STD effects between EI^{sc} and HPr^{sc} by observing the methyl region of HPr^{sc} (Fig. 2 *A*). Saturation times of 1.5 s were needed to fully saturate the upfield-shifted region of the protein (Fig. 2 *B*). The dissociation constant obtained by using different saturation times was 95 ± 30 μM (Fig. 2 *C*). This value was an order of magnitude higher than that obtained for binding of EI to HPr in *E. coli* (20,21), or *M. capricolum* (19). Because of spectral overlapping in the one-dimensional STD-NMR experiments and the absence of a complete assignment of the resonances of the intact protein, we could not identify the particular protons involved in the binding region.

Conversely, in HPr^{9-30}, we were able to identify which protons showed STD effects. The STD effects were observed in D_2O for the C_2H and C_4H protons of the His-15 (using the numbering of the intact protein) and the aromatic protons of Phe-22, which partially overlapped with those of Trp-10. The methyl protons of Leu-14, Ile-21, and Val-23 also showed intense STD effects, although we could not discriminate which methyl group (Fig. 3 *A*). As with HPr^{sc}, saturation times of 1.5 s were necessary to achieve a full protein signal saturation (Fig. 3 *B*). Among all protons experiencing saturation effects, the methyl groups showed the largest variation, and consequently, they were used to determine the K_D (Fig. 3 *C*). The obtained value for the K_D was 420 ± 90 μM, which was larger than that obtained for HPr^{sc} (see above).

It could be thought that the absence of the effectors would alter the affinity of the peptide by EI^{sc}. However, control experiments, with EI^{sc} in the presence of its effectors (4 mM Mg^{2+} and 2 mM PEP) showed that the signals of HPr^{9-30} also became broader, but there were no changes in the chemical shifts of the backbone, nor in the side-chain protons, nor in the magnitude of the STD effects (data not shown).

The CAC and thioredoxin control peptides did not show any STD effects. Conversely, the peptide found by phage display analysis (33) did show STD effects, especially with the aromatic and the methyl protons (data not shown), suggesting that even though it was designed against EI^{ec}, it could also bind to EI^{sc}. Thus, although the affinity of HPr^{9-30} for EI^{sc} is very small, it appears to be specific.

Binding of EI^{sc} to HPr^{9-30} and HPr^{sc} monitored by ITC

Data were analyzed by using a simple two-state model and with a 1:1 stoichiometry, as has been reported in other members of the HPr family (19,20) and used during analysis of the STD data (see above). The measured apparent dissociation constants agree reasonably well with those obtained by STD-NMR experiments: 120 ± 20 μM for the intact HPr^{sc}, and 230 ± 80 μM for HPr^{9-30} (Fig. 4, Table 1). (It could be thought that with those affinity constants, the complete saturation curve in the ITC experiments could be obtained with a 1 mM stock solution of peptide instead of the used stock solution of 0.3 mM of HPr^{9-30} (see Materials and Methods). In our experience, with peptides with weak affinities (such as those used as controls in this work), it would require peptide stock concentrations of 10 mM or larger to obtain a complete saturation curve. We have observed that the NMR spectrum of HPr^{9-30} at concentrations higher than 5 mM shows significant broadening, suggesting oligomerization reactions, whose order and equilibrium constants are unknown; then, the use of high concentrations in the stock peptide would require an additional reaction to estimate the affinity constant of the peptide for EI^{sc}. CD cannot be used either because of the large voltage in the detector at the concentrations required during the titration. Finally, the use of fluorescence was not possible because of the self-associating properties of the peptide indicated above and the large inner-filter effects at the concentrations needed in the experiment.)

To determine the buffer-independent enthalpy of the binding reaction, the effect of the buffer ionization heat was taken into account by carrying out the binding reaction in two buffers: Tris and MOPS, which have different ionization enthalpies (11.7 and 5.5 kcal mol^{-1}, respectively). With this procedure (35,36), the buffer-independent enthalpy of the binding reaction ΔH^0 was obtained, and the number of exchanged protons between the complex and the bulk solution, n_H, was calculated (Table 1). A positive value of n_H indicates a protonation, the uptake of a proton by the complex (such as

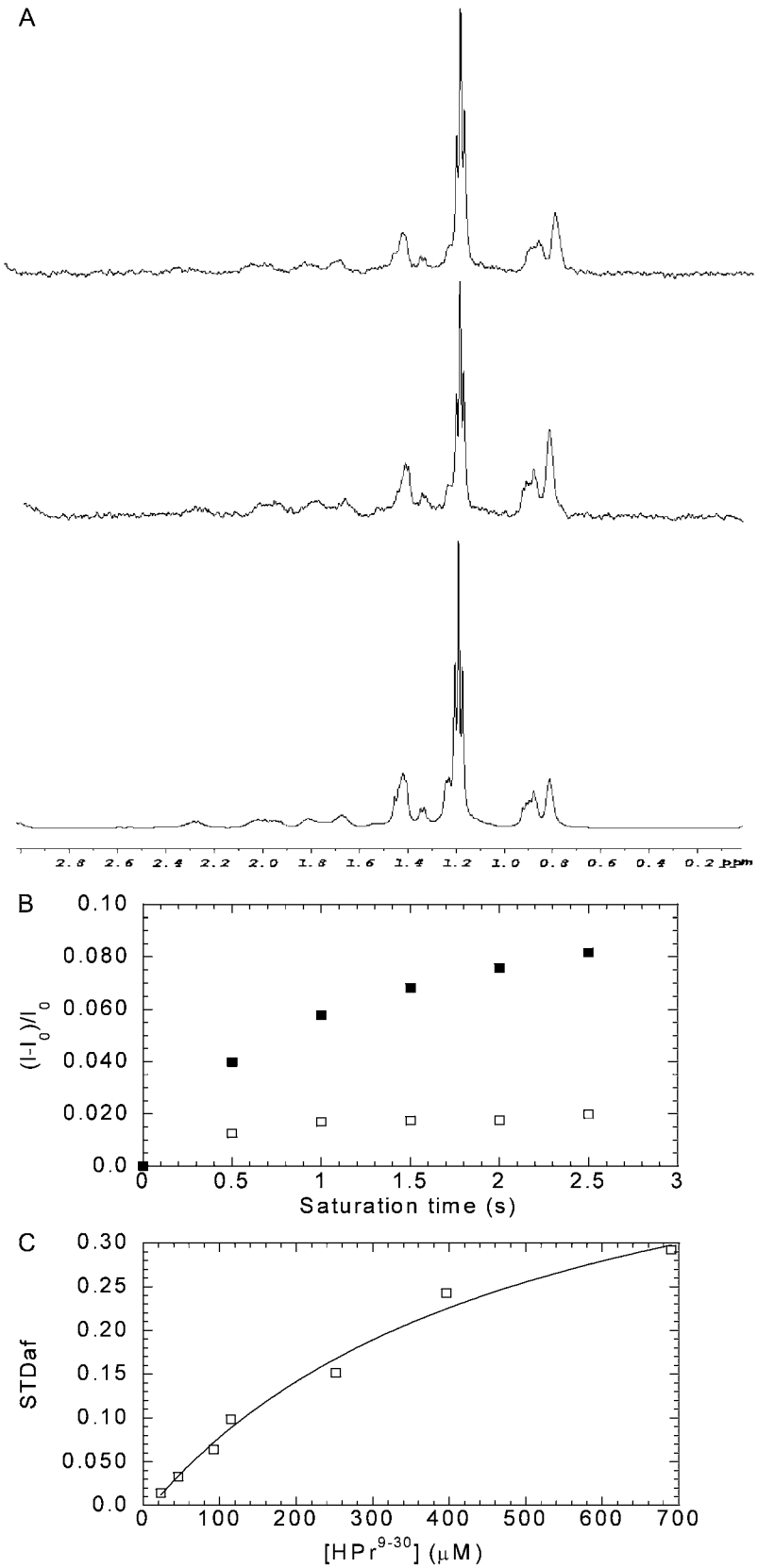

FIGURE 3 Binding of EI^{sc} to HPr$^{9–30}$ measured by STD-NMR. (*A*) STD-NMR spectra at different saturation times, from bottom to top: reference spectrum (*bottom*), STD spectrum at 1 s of saturation (*middle*), and at 2 s of saturation (*top*). (*B*) The rate between the methyl peak intensity in the STD spectra and that at the reference spectrum at 46.0 μM (*open squares*) and at 115.0 μM of HPr^{sc} (*solid squares*). (*C*) Binding curve for the *STDaf* of the methyl signals in HPr$^{9–30}$ at 2 s of saturation time. The curve is the fitting of data to the equation of *STDaf*. Conditions were: 8.6 μM of EI^{sc} at 283 K.

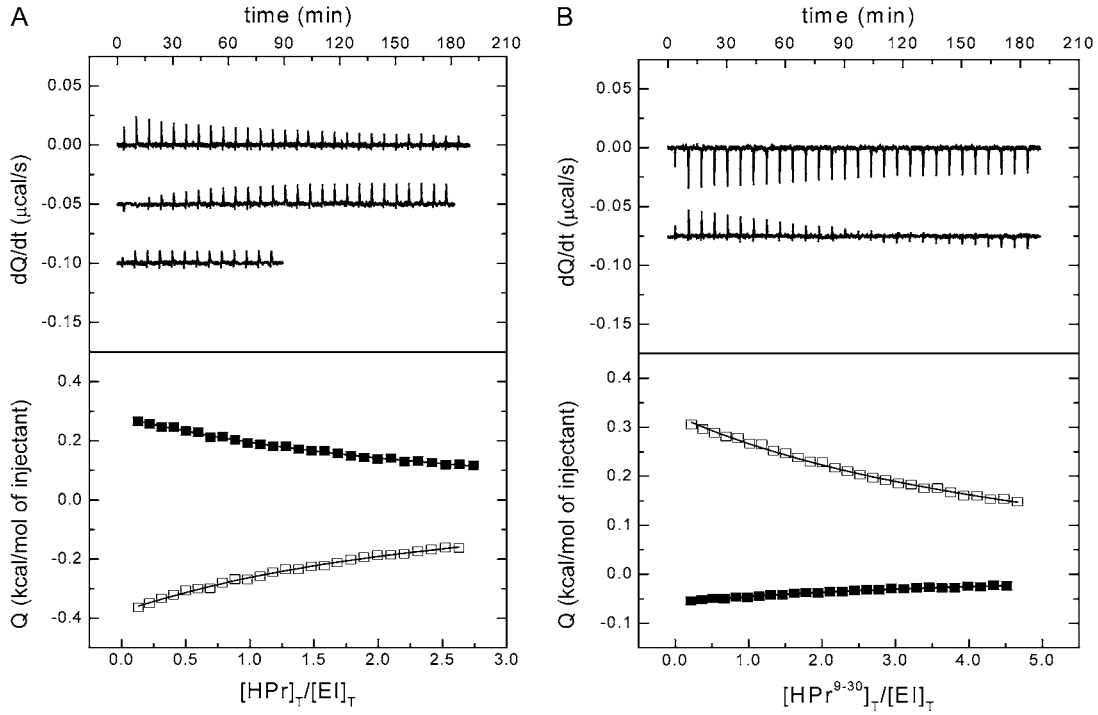

FIGURE 4 ITC measurements. (*A*) HPr binding to EI^{sc}. The top trace shows the raw data, and the lower trace is the fitting after signal integration. The short sequence of raw data is a control experiment (the last data in the *upper left panel*), where the individual heats of dilution for HPr^{sc} were determined under the same experimental conditions by making identical injections of the HPr^{sc} solution into the titration cell, which contained only buffer. Measurements were carried out in 12 mM Tris with 100 mM NaCl (*solid squares*) and 12 mM MOPS with 100 mM NaCl (*open squares*). (*B*) HPr^{9-30} binding to EI^{sc}. The traces and the buffers used are the same as those described in HPr^{sc}.

happens with the complex between EI^{sc} and the intact HPr^{sc}, where the number of exchanged protons is 1); on the other hand, a negative value of n_H indicates a deprotonation, the release of a proton from a residue in the complex (such as in HPr^{9-30}, where the number of exchanged protons is -1).

TABLE 1 Binding parameters of the association reaction of EI with HPr and with HPr^{9-30}

Thermodynamic parameter	HPr	HPr^{9-30}
K_D (μM) *	95 ± 30	420 ± 90
K_D (μM)	120 ± 20	230 ± 80
$\Delta H_{mea,Tris}$ (kcal mol^{-1})	1.9 ± 0.4	−0.7 ± 0.2
$\Delta H_{mea,MOPS}$ (kcal mol^{-1})	−2.5 ± 0.4	5.1 ± 0.4
ΔH^0 (kcal mol^{-1})†	−6.3 ± 0.6	10.2 ± 0.4
ΔG^0 (kcal mol^{-1}) ‡	−5.4 ± 0.2	−4.8 ± 0.2
$-T\Delta S^0$ (kcal mol^{-1}) §	−0.9 ± 0.6	−15.0 ± 0.4
n_H	0.72	−0.96

As determined by ITC at 298 K; K_D is the dissociation constant.
*As determined by STD-NMR at 283 K. The values shown are the average of the dissociation constant obtained at saturation times of 2.5, 2, 1.5, and 1 s; the error is the standard deviation.
†It is the value of the enthalpy for the binding reaction.
‡Determined as $\Delta G^0 = RT\ln K_D$. The average of the values obtained by STD-NMR and ITC measurements is reported.
§Determined as $-T\Delta S^0 = \Delta G^0 - \Delta H^0$.

DISCUSSION

The region of HPr^{9-30} that interacts with EI^{sc} is the same as in the intact HPr

In the solution structure of the complex between the N-terminal domain of EI^{ec} and HPr^{ec} (17), there are hydrophobic contacts involving residues in the first α-helix of HPr^{ec} (within parentheses the corresponding residue in HPr^{sc}), namely, Thr-16 (Ala-16), Arg-17, and Ala-20 (Ser-20). Further, the side chain of Arg-17, a residue conserved in other HPrs, is involved in salt bridges with other residues within EI^{ec} (17). The environments of His-15, Gln-21 (Ile-21) and Val-23 were also modified, as shown by the changes in the chemical shifts of some of their protons (18). Similarly, the residues of HPr^{ec}, belonging to the first helix, that show interactions with the glucose-specific enzyme IIA, are Leu-14, Thr-16 (Ala-16), Gln-21 (Ile-21), and Val-23; and those showing interactions with glycogen phosphorylase are Ala-10 (Trp-10), Gly-13, Ala-19, and Ala-20 (Ser-20) (18). The most affected regions of HPr on binding to EI or other proteins, then, were clustered in the region contained in the designed HPr^{9-30}.

The most important STD effects in HPr^{9-30} were observed in the side chains of Leu-14, the active-site His-15, Ile-21 (Gln-21 in HPr^{ec}), and Val-23. We could not unambiguously detect STD effects in the rest of the aliphatic chains of the

residues affected because severe overlapping exists in the alkyl region (26). However, from the above pieces of evidence, we suggest that HPr^{9-30} acquires a native-like conformation on binding to EI^{sc} because otherwise those residues could not show the STD effects measured (vide infra).

The affinity of HPr^{9-30} for EI^{sc} is smaller than that of the intact HPr^{sc}

The observed dissociation constant for HPr^{9-30} was only two-and-a-half times larger than that of the intact HPr^{sc} (Table 1), as shown by ITC and STD-NMR measurements. The observed binding affinity for the HPr^{9-30} is an apparent binding constant modulated by the conformational change toward a native α-helical conformation coupled to the binding process. The HPr^{9-30} fragment is disordered in solution (26), and it must adopt (as suggested by the STDs) a native-like conformation when it binds to EI^{sc}, resulting in a free energy penalty associated with such a conformational transition. From TFE conformational equilibrium experiments of HPr^{9-30} (26), a free energy difference of 2.7 kcal mol^{-1} in aqueous solution has been estimated between the disordered and its native-like helical structure; this value yields an equilibrium constant of $K = [N]/[U] = 0.011$ for the conformational change, where N is the helical native-like conformation, and U is the unfolded conformation of the peptide. (This equilibrium constant is obtained by using the linear extrapolation method in the changes of the ellipticity at 222 nm of HPr^{9-30} as TFE concentration is varied. Thus, the free energy of the peptide folding reaction ($U \rightleftarrows N$) follows $\Delta G = \Delta G^0 + m$ [TFE], where ΔG^0 is the free energy of the reaction in the absence of TFE (see Hurtado-Gómez et al. (26) for details).) The apparent binding constant is equal to $K_L/(1 + K^{-1})$, where K_L is the intrinsic binding constant in the absence of the coupled conformational equilibrium in the peptide. Therefore, the observed binding affinity should be corrected by a factor of 90 or slightly less to estimate the intrinsic binding affinity of the fragment (it would be lower if the isolated HPr^{9-30} showed some residual structure, which could be too fast to be detected by NMR techniques). Conversely, binding between HPr^{sc} and EI^{sc} should not result in large conformational changes, as shown by the NMR structures of the complex in *E. coli* (17,18). Then, the intrinsic binding affinity of the fragment appears to be higher than that of the intact HPr^{sc}, and therefore, HPr^{9-30} may represent an excellent template for ligand optimization. This result is somewhat surprising because the peptide contains only 22 residues of the intact protein, but it is encouraging because it proves that most of the crucial residues for binding are those contained in the fragment. With the phage display, several peptides designed against EI^{ec} have shown cell growth inhibition (33), but no clue about the corresponding mechanism has been provided. The peptides share similar residues with HPr^{9-30}, and we suggest that the inhibition of the whole PTS system in vitro by the phage peptides results from interaction with EI.

On the other hand, the buffer-independent binding enthalpies and the number of exchanged protons are also markedly different when intact HPr^{sc} and HPr^{9-30} bind to EI^{sc}. However, if we keep in mind the conformational changes undergone by the small fragment when it binds to EI^{sc}, these differences are not unexpected. The association reaction in HPr^{sc} has a negative enthalpy value (Table 1); then, with that measured K_D, the entropy change to compensate ΔG should be small and negative; that is, the reaction should be enthalpy-driven. In contrast, when HPr^{9-30} is bound to EI^{sc}, the value of the enthalpy is positive, suggesting that the entropy contribution should be large and positive (entropy-driven). Because the fragment acquires a native folded conformation on binding, we could explain this positive entropy value in terms of the balance between a conformational entropy decrease and a desolvation entropy increase on fragment folding; in addition, other contributions to the entropy change need to be considered (such as deprotonation of ionizable groups).

Some comments, however, must be made about the ITC experiments and their possible drawbacks. Because the binding affinity is low, the stoichiometry, n, must be fixed in the nonlinear square-fitting procedure. When the affinity is low, it is not possible to estimate affinity, enthalpy, and stoichiometry independently by ITC, and a value for the stoichiometry must be assumed. The natural election, in the absence of additional information, is $n = 1$; that is, there is one binding site with a protein completely pure (as checked by SDS-PAGE) and binding-competent. However, this is a limitation inherent to any binding technique, not only for ITC. In fact, the equation used to estimate the dissociation constant by STD-NMR is the very well known and widely employed equation for ligand binding analysis where it is implicitly assumed that the stoichiometry is $n = 1$. Of course, the assumption of a fixed value for the stoichiometry will condition the accuracy of the enthalpy estimation, but the affinity determined will not be much affected by the election of the stoichiometry value. However, using the same value for the stoichiometry in all experiments will make the enthalpy error homogeneous; as a rule of thumb, an error of 20% in the stoichiometry will produce an error of 20–25% in the enthalpy of a low-affinity equilibrium. Then, the discussion about the binding energetics of HPr^{sc} and its fragment is valid even with an error of 20% in the enthalpy.

The idea of estimating the buffer-independent enthalpy is to eliminate the possible influence of the buffer on the value of the measured enthalpy. Two buffers were employed just to have a rough estimate of this parameter. Because the observed values of the enthalpy for each buffer may be affected by 20% error (as a result of the stoichiometry error mentioned above), it is worthless to refine the linear regression fitting by using more than two buffers. Even with the possible errors in the enthalpy values, it is clear that the buffer-independent enthalpy must be negative for HPr and positive for its fragment, because in both cases the enthalpy determined in MOPS and the enthalpy determined in Tris are of opposite

sign. Something similar happens with the net number of exchanged protons: it must be positive for HPr and negative for its fragment.

The magnitude of the heats is fairly small, as expected for a reaction with low affinity and low enthalpy. However, a control experiment was carried out by injecting ligand into buffer, and equal constant heats were obtained (shown in Fig. 4). Therefore, the decreasing/increasing heats obtained in the titrations with protein and ligand must reflect the binding process.

Thus, the ITC experiments may serve as a confirmation of the weak affinity determined by STD. In addition, even taking into account certain significant errors in the enthalpy values determined (directly measured and buffer-independent), they make it possible to detect thermodynamic differences in the binding of HPr^{sc} or its fragment to EI^{sc} (the enthalpy value and the net number of exchanged protons are of opposite sign) that may reflect differences in the mode of binding of both ligands. These differences are not as clear when only the binding affinities, which are not as different, are compared.

The affinity of HPr^{sc} for its EI^{sc} partner is smaller than in other members of the HPr family

One of the results of this study is that in *S. coelicolor*, the dissociation constant for the EI^{sc}:HPr^{sc} is larger ($\sim$100 μM) than those measured in *E. coli* (9 μM) or *M. capricolum* (7 μM) (19,20). It can be thought that there are three possible reasons to explain such discrepancy. First, because EI is a dimer, the different amount of EI used for each species could account for the discrepancies; however, the concentrations used in this work were similar (10 μM) to those used in the experiments with *E. coli* and *M. capricolum* (19,20) ($\sim$30 μM). Alternatively, because the dimerization state of EI^{ec} has been shown recently to be exquisitely dependent on the solution conditions (37), we could think that under our conditions EI^{sc} was not dimeric, and then, it could result in a lower affinity constant for HPr^{sc}. We have previously shown that dimerization of EI^{sc} can be monitored by fluorescence quenching (12), and then we have extended here the range of explored protein concentrations. The dominant EI^{sc} species was dimeric within the protein concentration range used in this work (8 to 12 μM), and the lower affinity for HPr^{sc} cannot be attributed to the presence of a significant population of monomeric EI^{sc} species.

Second, the binding affinity could be affected by the buffer used in the titration. The buffers used in *S. coelicolor* in this work were phosphate (for STD-NMR), MOPS, and Tris (for ITC measurements); in other HPr species studied, the phosphate buffer was chosen (19–21). Because even when different buffers are used, the different techniques used in this work, yield similar dissociation constants, so the discrepancy observed among the affinities in the different species cannot be caused by the buffers. Besides, the measured binding affinity is not affected by the buffer used as long as the pK_a of the buffer is close to the pH of the solution and the buffer itself does not interact specifically with any of the interacting molecules. Very briefly, if, for instance, the binding involves a protonation of an ionizable group and, therefore, a deprotonation of the buffer to keep the pH constant, the equilibrium constant of the overall reaction is $K = [MLH^+][B^-]/[M][L][BH]$, which does not depend on the buffer if the concentration of base and acid forms are equal (that is, if the pH is equal to the buffer pK_a). In contrast, the measured binding enthalpy by ITC will always contain a contribution from buffer ionization (protonation or deprotonation) if there is a net proton exchange between the complex and the bulk solution. This net exchange is caused by a pK_a change on binding in certain ionizable groups elicited by a change in their solvation microenvironment. For that reason, the buffer-independent enthalpy must be calculated from a set of experiments performed at the same conditions using buffers with different ionization enthalpies. The buffer-independent enthalpy will be composed of the intrinsic binding enthalpy (that is, the overall enthalpy as a result of the net balance between formation/breakdown of van der Waals, electrostatic, and hydrogen-bond interactions between the binding partners and the solvent) plus the ionization enthalpy of the groups involved in the proton exchange from the two binding partners. Previous studies did not correct for this ionization enthalpy, and our value (-6 kcal mol^{-1}) is different from those in other species (6 kcal mol^{-1} in *E. coli* and 5 kcal mol^{-1} in *M. capricolum* (19–21)). Thus, the binding reaction between EI^{sc} and HPr^{sc} is enthalpy-driven and in other species is entropy-driven. Because the structure of the intact HPr members seems to be similar, we do not know the exact reasons for this difference in the thermodynamic parameters, and they might rely on the different binding interfaces between EI:HPr complexes among the species (see below).

Finally, the binding of either the intact HPr^{sc} or HPr^{9-30} to EI^{sc} could be nonspecific in light of the small value of the affinity constant. At this stage, we can rule out that possibility because a control peptide, designed against inhibition of EI^{ec} (33), also binds to EI^{sc}, whereas two peptides designed against two different proteins, with no structural or sequence relationship to EI^{sc}, did not show binding to EI^{sc} (data not shown). Then, although binding in the *S. coelicolor* PTS is very weak, it is specific. These weak interactions are not strange at all in cells because, when locally enriched or involved in large multisubunit assemblies (as in HPr^{sc}), they may play key roles in many important cellular events (38). For instance, interactions between lymphocyte cell surface molecules are of the order of 10^{-4} to 10^{-6} M and are necessary for reversible cell-cell adhesion processes (39); furthermore, some hit compounds designed against particular protein-protein interfaces are in the range of the values of the affinity constants determined here for HPr^{sc} and HPr^{9-30} (40). Finally, it is interesting to note that weak interactions involving proteins do not occur only with other proteins and/or peptides but have also been observed in protein-lipid systems (41).

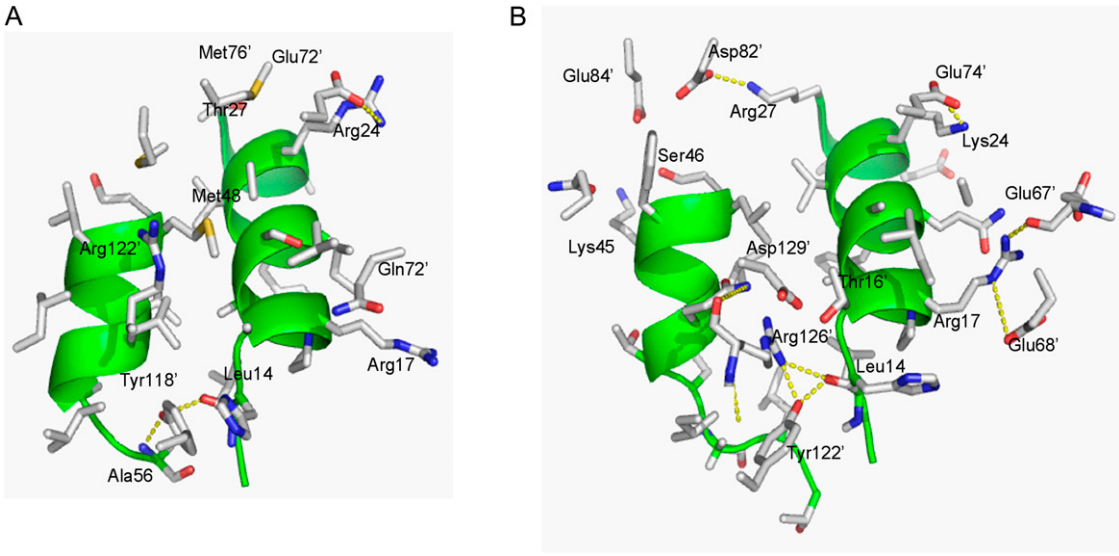

FIGURE 5 Interactions in the interface region of the complex between EIN and HPr. (*A*) Interface of the complex between the N-terminal domain of EI^{sc} and HPr^{sc} from the complex modeled by using Swiss-PDB-Viewer software and Swiss-Model Server (47). The model was obtained as described (12) with the structure of HPr (PDB number: 1PCH) used as a template. In the model, the Tyr-118 (of the N-terminal domain of EI^{sc}) is hydrogen-bonded to Ala-56 and Leu-14. (*B*) Interface of the NMR complex (17) between the N-terminal domains of EI^{ec} and HPr^{ec}. In both figures, the structural motifs of the binding region of HPr (two helical patches) are shown as green ribbons, and the side chains of the corresponding residues in sticks. The residues belonging to the binding region in the N-terminal domain of EI are shown as sticks, and the names of the corresponding residues are indicated with a prime. The color code of the atoms is: C (*gray*), O (*red*), N (*blue*), and S (*yellow*). The hydrogen bonds are shown as yellow dashed lines. The main chains, which were not involved in direct interactions and/or intrachain hydrogen bonds, are not shown.

There are, however, three reasons that could explain the discrepancy among our K_D and those previously reported (19–21), and, in addition, they might provide insights into the different values measured for the enthalpies among the different species. First, because there is a net proton exchange between the complex and the bulk solution on binding, the binding parameters are pH dependent. According to the value of n_H, a positive value indicates that the binding affinity will increase at lower pH, and it will decrease at higher pH. The measurements described in *E. coli* were carried out at pH 6.5, and those in *M. capricolum* at pH 7.5 (19,20). Second, we compared the structure of the complex between the N terminus of EI^{ec} and the HPr^{ec} (17) (Protein Data Bank 3EZE) with a model built for that complex between EI^{sc} and HPr^{sc} (Fig. 5). The interface of the complex in *E. coli* has a larger number of interactions (electrostatic and hydrogen-bonds) than that of the modeled complex. Then, because a larger number of interactions usually leads to a stronger affinity, we may conclude that the affinity (and then the stability) of the EI:HPr complex will be lower in *S. coelicolor* than in *E. coli*. And finally, EI is a dimer, but the EI protein in any species must be in the monomeric form to bind HPr (42–45). Its dissociation constant is, in all the measured species so far, in the range of micromolar at room temperature, except, in *Salmonella typhyimurium*, where it reaches a nanomolar value at 296 K (46); however, we have estimated that the dissociation constant of EI^{sc} at 298 K must be lower than 1 μM under our conditions (12), and then, lower than that of EI^{ec}. Therefore, the interaction strength in the dimer is larger in EI^{sc}, and even if the intrinsic binding affinities in EI^{sc} and the EI^{ec} for their corresponding HPr proteins were the same, the apparent affinity of HPr toward EI would be lower in *S. coelicolor*. It is interesting to note, however, that peptides against EI^{ec} (33) also bind to EI^{sc} (one of our control peptides, see above). Then, because the binding interfaces are so different among the bacterial species, we envisage that the phosphorylation of sugars in *S. coelicolor* could be hampered in the future by using modifications of HPr^{9-30}, with a larger affinity than that described here. However, peptides or peptide derivatives, which could be used interspecies, would need a larger and more careful design and should be tested against the different species.

We thank the two anonymous reviewers for their suggestions and invaluable criticisms. We thank Prof. Manuel Rico for careful reading and corrections of the manuscript and Dr. Francisco N. Barrera for reading the manuscript and helpful suggestions.

This work has been supported by grants SAF2004-07722 (to A.V.-C. and O.A.), CTQ2005-00360/BQU (to J.L.N.), and CTQ2006-09052 (to M.J.H.) from the Spanish Ministry of Education and Science. A.V.-C. is a recipient of a Ramon y Cajal Research Contract from the Spanish Ministry of Science and Technology. E.H.-G. was recipient of a Ph.D. fellowship from Generalitat Valenciana. The authors declare they do not have any competing interest.

REFERENCES

1. Levy, S. B., and B. Marshall. 2004. Antibacterial resistance worldwide: causes, challenges and responses. *Nat. Med.* 10:S122–S129.

2. Payne, D. J., M. N. Gwynn, D. J. Holmes, and D. L. Pompliano. 2007. Drugs for bad bugs: confronting the challenges of antibacterial discovery. *Nat. Rev. Drug Discov.* 6:29–40.
3. Postma, P. W., J. W. Lengeler, and G. R. Jacobson. 1993. Phosphoenolpyruvate carbohydrate phosphotransferase systems of bacteria. *Microbiol. Rev.* 57:543–594.
4. Brückner, R., and F. Titgemeyer. 2002. Carbon catabolite repression in bacteria: choice of the carbon source and autoregulatory limitation of sugar utilization. *FEMS Microbiol. Lett.* 209:141–148.
5. Ginsburg, A., and A. Peterkofsky. 2002. Enzyme I: the gateway to the bacterial phosphoenolpyruvate:sugar phosphotransferase system. *Arch. Biochem. Biophys.* 397:273–278.
6. Bentley, S. D., K. F. Chater, A. M. Cerdeno-Tarraga, G. L. Challis, N. R. Thomson, K. D. James, D. E. Harris, M. A. Quail, H. Kieser, D. Harper, A. Bateman, S. Brown, G. Chandra, C. W. Chen, M. Collins, A. Cronin, A. Fraser, A. Goble, J. Hidalgo, T. Hornsby, S. Howarth, C. H. Huang, T. Kieser, L. Larke, L. Murphy, K. Oliver, S. O'Neil, E. Rabbinowitsch, M. A. Rajandream, K. Rutherford, S. Rutter, K. Seeger, D. Saunders, S. Sharp, R. Squares, S. Squares, K. Taylor, T. Warren, A. Wietzorrek, J. Woodward, B. G. Barrell, J. Parkhill, and D. A. Hopwood. 2002. Complete genome sequence of the model actinomycete *Streptomyces coelicolor* A3(2). *Nature.* 417:141–147.
7. Parche, S., R. Schmid, and F. Titgemeyer. 1999. The PTS system of *Streptomyces coelicolor*: identification and biochemical analysis of a histidine phosphocarrier protein HPr encoded by the gene ptsH. *Eur. J. Biochem.* 265:308–317.
8. Nothaft, H., D. Dresel, A. Willimek, K. Mahr, M. Niederweis, and F. Titgemeyer. 2003. The phosphotransferase system of *Streptomyces coelicolor* is biased for N-acetylglucosamine metabolism. *J. Bacteriol.* 185:7019–7023.
9. Fernández-Ballester, G., J. Maya, A. Martin, S. Parche, J. Gómez, F. Titgemeyer, and J. L. Neira. 2003. The histidine-phosphocarrier protein of *Streptomyces coelicolor* folds by a partially folded species at low pH. *Eur. J. Biochem.* 270:2254–2267.
10. Neira, J. L., and J. Gómez. 2004. The conformational stability of the *Streptomyces coelicolor* histidine-phosphocarrier protein. Characterization of cold denaturation and urea-protein interactions. *Eur. J. Biochem.* 271:2165–2181.
11. Hurtado-Gómez, E., F. N. Barrera, and J. L. Neira. 2005. Structure and conformational stability of the enzyme I of *Streptomyces coelicolor* explored by FTIR and circular dichroism. *Biophys. Chem.* 115:229–233.
12. Hurtado-Gómez, E., G. Fernández-Ballester, H. Nothaft, J. Gómez, F. Titgemeyer, and J. L. Neira. 2006. Structure, association and conformational stability of the Enzyme I of the *Streptomyces coelicolor* phosphoenolpyruvate: sugar phosphotransferase system. *Biophys. J.* 90:4592–4604.
13. Van Nuland, N. A. J., I. W. Hangyi, R. C. Van Schaik, H. J. C. Berendsen, W. F. Van Gusteren, R. M. Scheek, and G. T. Robillard. 1994. The high-resolution structure of the histidine-containing phosphocarrier protein HPr from *Escherichia coli* determined by restrained molecular dynamics from nuclear magnetic resonance nuclear Overhauser effect data. *J. Mol. Biol.* 237:544–559.
14. Maurer, T., R. Doker, A. Gorler, W. Hengstenberg, and H. R. Kalbitzer. 2001. Three-dimensional structure of the histidine-containing phosphocarrier protein (HPr) from *Enterococcus faecalis* in solution. *Eur. J. Biochem.* 268:635–644.
15. Herzberg, O., P. Reddy, S. Sutrina, M. H. Saier, Jr., J. Reizer, and G. Kapadia. 1992. Structure of the histidine-containing phosphocarrier protein HPr from *Bacillus subtilis* at 2.0-Å resolution. *Proc. Natl. Acad. Sci. USA.* 89:2499–2503.
16. Jia, Z., J. W. Quail, E. B. Waygood, and L. T. J. Delbaere. 1993. The 2.0-Å resolution structure of *Escherichia coli* histidine-containing phosphocarrier protein HPr: a redetermination. *J. Biol. Chem.* 268: 22490–22501.
17. Garrett, D. S., Y. J. Seok, A. Peterkofsky, A. M. Gronenborn, and G. M. Clore. 1999. Solution structure of the 40,000 Mr phosphoryl transfer complex between the N-terminal domain of enzyme I and HPr. *Nat. Struct. Biol.* 6:166–173.
18. Wang, G., M. Sondej, D. S. Garret, A. Peterkofsky, and G. M. Clore. 2000. A common interface on histidine-containing phosphocarrier protein for interaction with its partner proteins. *J. Biol. Chem.* 275:16401–16403.
19. Zhu, P.-P., R. H. Szczepanowski, N. J. Nosworthy, A. Ginsburg, and A. Peterkofsky. 1999. Reconstitution studies using the helical and carboxy-terminal domains of enzyme I of the phosphoenolpyruvate: sugar phosphotransferase system. *Biochemistry.* 38:15470–15479.
20. Chauvin, F., A. Fomenkov, C. R. Johnson, and S. Roseman. 1996. The N-terminal domain of *Escherichia coli* enzyme I of the phosphoenolpyruvate/glycose phosphotransferase system: molecular cloning and characterization. *Proc. Natl. Acad. Sci. USA.* 93:7028–7031.
21. Ginsburg, A., R. H. Szczepanowski, S. B. Ruvinov, N. J. Nosworthy, M. Sondej, T. C. Umland, and A. Peterkofsky. 2000. Conformational stability changes of the amino terminal domain of enzyme I of the *Escherichia coli* phosphotransferase system produced by substituting alanine or glutamate for the active-site histidine 189: implications for phosphorylation effects. *Protein Sci.* 9:1085–1094.
22. Pace, C. N., and J. M. Scholtz. 1997. How to determine the molar absorbance coefficient of a protein. *In* Protein Structure, 2nd ed. T. E. Creighton, editor. 253–259, Oxford University Press, New York. 253–259.
23. States, D. J., R. A. Haberkorn, and D. J. Ruben. 1982. A two-dimensional nuclear Overhauser experiment with pure absorption phase in four quadrants. *J. Magn. Reson.* 48:286–292.
24. Piotto, M., V. Saudek, and V. Sklenar. 1992. Gradient-tailored excitation for single-quantum NMR spectroscopy of aqueous solutions. *J. Biomol. NMR.* 2:661–665.
25. Bax, A., and D. G. Davis. 1985. MLEV-17 based two-dimensional homonuclear magnetization transfer spectroscopy. *J. Magn. Reson.* 65:355–360.
26. Hurtado-Gómez, E., M. Caprini, A. Prieto, and J. L. Neira. 2007. The helical structure propensity in the first helix of the histidine phosphocarrier protein of Streptomyces coelicolor. *Protein Pept. Lett.* 14:281–290.
27. Mayer, M., and B. Meyer. 1999. Characterization of ligand binding by saturation transfer difference NMR spectroscopy. *Angew. Int. Chem. Int. Ed.* 38:1784–1788.
28. Mayer, M., and B. Meyer. 2001. Group epitope mapping by saturation transfer difference NMR to identify segments of ligand in direct contact with protein receptor. *J. Am. Chem. Soc.* 123:6108–6117.
29. Klein, J., R. Meinekee, M. Mayer, and B. Meyer. 1999. Detecting binding affinity to immobilized receptor proteins in compound libraries by HR-MAS STD NMR. *J. Am. Chem. Soc.* 121:5336–5337.
30. Yan, J., A. D. Kline, H. Mo, M. J. Shapiro, and E. R. Zartler. 2003. The effect of relaxation on the epitope mapping by saturation transfer difference NMR. *J. Magn. Reson.* 163:270–276.
31. Prost, E., P. Sizun, M. Piotto, and J. M. Nuzillard. 2002. A simple scheme for the design of solvent-suppression pulses. *J. Magn. Reson.* 159:76–81.
32. Meyer, B., and T. Peters. 2003. NMR spectroscopy techniques for screening and identifying ligand binding to protein receptors. *Angew Int. Chem. Int. Ed.* 42:864–890.
33. Mukhija, S., and B. Erni. 1997. Phage display selection of peptides against enzyme I of the phosphoenolpyruvate-sugar phosphotransferase system (PTS). *Mol. Microbiol.* 25:1159–1166.
34. Garzón, M. T., M. C. Lidón-Moya, F. N. Barrera, A. Prieto, J. Gómez, M. G. Mateu, and J. L. Neira. 2004. The dimerization domain of the HIV-1 capsid protein binds a capsid protein-derived peptide. *Protein Sci.* 13:1512–1523.
35. Gómez, J., and E. Freire. 1995. Thermodynamic mapping of the inhibitor site of the aspartic protease endothiapepsin. *J. Mol. Biol.* 252:337–350.
36. Neuwirth, M., K. Flicker, M. Strohmeier, I. Tews, and P. Macheroux. 2007. Thermodynamic characterization of the protein-protein interaction in the heteromeric *Bacillus subtilis* pyridoxalphosphate synthase. *Biochemistry.* 46:5131–5139.
37. Patel, H. V., K. A. Vyas, R. Savtchenko, and S. Roseman. 2006. The monomer/dimer transition of enzyme I of the *Escherichia coli* phosphotransfrase system. *J. Biol. Chem.* 281:17570–17578.

38. Nooren, I. M., and J. M. Thornton. 2003. Diversity of protein-protein interactions. *EMBO J*. 22:3486–3492.

39. van der Merwe, P. A., and S. J. Davis. 2003. Molecular interactions mediating T cell antigen recognition. *Annu. Rev. Immunol*. 21: 659–684.

40. Wells, J. A., and C. L. McClendon. 2007. Reaching for high-hanging fruit in drug discovery at protein-protein interfaces. *Nature*. 450:1001–1009.

41. Chen, K., I. Bachtiar, G. Piszczek, F. Bouamr, C. Carter, and N. Tjandra. 2008. Solution NMR characterization and dynamics of equine infectious anaemia virus matrix protein and its interaction with PIP2. *Biochemistry.* 47:1928–1937.

42. Meadow, N. D., R. L. Mattoo, R. S. Savtchenko, and S. Roseman. 2005. Transient state kinetics of enzyme I of the phosphoenolpyruvate: glycose phosphotransferase system of *Escherichia coli*: equilibrium and second order rate constants for the phosphotransfer reactions with phosphoenolpyruvate and HPr. *Biochemistry*. 44:12790–12796.

43. Chauvin, F., L. Brand, and S. Roseman. 1994. Sugar transport by the bacterial phosphotransferase system. Characterization of the *Escherichia coli* enzyme I monomer/dimer transition kinetics by fluorescence anisotropy I. *J. Biol. Chem.* 269:20263–20269.

44. Chauvin, F., L. Brand, and S. Roseman. 1994. Sugar transport by the bacterial phosphotransferase system. Characterization of the *Escherichia coli* enzyme I monomer/dimer transition kinetics by fluorescence anisotropy II. *J. Biol. Chem.* 269:20270–20274.

45. Dimitrova, M. N., R. H. Szczepanowski, S. B. Ruvinov, A. Peterkofsky, and A. Ginsburg. 2002. Interdomain interaction and substrate coupling effects of dimerization and conformational stability of Enzyme I of the *Escherichia coli* phosphoenolpyruvate:sugar phosphotransferase system. *Biochemistry.* 41:906–913.

46. Kukuruzinska, M. A., B. W. Turner, G. K. Ackers, and S. Roseman. 1984. Subunit association of enzyme I of the *Salmonella typhimurium* phosphoenolpyruvate:glycose phosphotransferase system: temperature dependence and thermodynamic properties. *J. Biol. Chem.* 259:11679–11682.

47. Guex, N., and M. C. Peitsch. 1997. Swiss-model and the Swiss-PDB viewer: an environment for comparative protein modelling. *Electrophoresis.* 18:2714–2723.